

Lasers in Manufacturing Conference 2015

# Analysis and Optimization of Process Parameters in Al-SiCp Laser Cladding.

A. Riquelme<sup>a\*</sup>, P. Rodrigo<sup>a</sup>, M.D. Escalera<sup>a</sup>, J.Rams<sup>a</sup>

<sup>a</sup> *Department of Materials Science and Technology. School of Experimental Sciences and Technology. Rey Juan Carlos University. C/ Tulipán s/n; 28933 Móstoles. Spain.*

---

## Abstract

The process parameters of the laser cladding have great effect on the clad geometry and dilution of the single and multi-pass coatings of an aluminum matrix composite reinforced with SiC particles (Al/SiCp) on ZE41 magnesium alloys using a high-power diode laser (HPLD). The influence of the laser power (500-700 W), scanning speed (3-17 mm/s) and focal position of the laser beam (focus, positive and negative defocus) on the shape factor, the cladding-bead geometry, the cladding-bead microstructure including the presence of pores and cracks, and mechanical properties such as hardness has been evaluated. From the measured values, different contour maps were produced, which show the correlation of these process parameters and their influence on the properties and ultimately, with the feasibility of the cladding process. The importance of the focal position is demonstrated. The different energy distribution of the cross section of the laser beam in focus, positive and negative defocus affects on the cladding-bead properties.

Keywords: Macro Processing, Laser Cladding, focal position, laser parameters.

---

## 1. Introduction.

Laser cladding is an effective and easy fabrication process to obtain composite coatings, in that, compared to conventional methods like thermal spraying or arc welding, the surface layers obtained by laser cladding technique have higher mechanical properties, good metallurgic bonding and low metallurgic defects (Zhong et al., 2010). A number of studies have been conducted to investigate the influences of process

---

\* Corresponding author. Tel.: +34-91-4888252; fax: +34-91-4888150.  
E-mail address: ainhoa.riquelme.aguado@urjc.es

parameters on laser cladding properties, but each application requires the appropriate selection of the laser cladding process to satisfy its particular needs (Liu et al., 2006; Lee, 2008; Sun et al., 2012; Gao et al., 2014).

Magnesium and aluminum alloys are attracting high attention due to their reduced density, which provides them high specific values of stiffness and strength. This combined with a great facility of processing and reasonable cost, makes them suitable for application in many sectors and especially in the transportation one. Nevertheless, the use of magnesium and aluminum alloys is limited because of their low superficial properties. The modification of the superficial properties of these alloys would allow extending the applications where they can be used. The addition of zinc to magnesium significantly improves the strength of both cast and wrought alloys. In particular, the alloys containing Zn and rare earths (RE), such as the ZE41 used in this work, have moderate strength and creep resistance combined with good castability (Avedesian and Baker, 1999). Aluminium matrix composites reinforced with ceramic particles have received considerable attention due to the combination of their tribological properties without sacrificing the corrosion resistance of aluminum alloys (Hooker and Doorbar, 2000). These composites are currently being developed for various applications, such as, pistons and cylinder liners in automotive engines (Shibata and Ushio, 1994). SiC, B<sub>4</sub>C, Al<sub>2</sub>O<sub>3</sub> and TiC in the shape of particles are excellent reinforcement materials for Al-MMC, due to their high hardness and chemical and thermal stabilities, although carbides, in particular SiCp (SiC particles), tend to react and dissolve in molten aluminum at high temperatures and form Al<sub>4</sub>C<sub>3</sub> which have a hygroscopic nature (Ureña et al., 2009).

In this work, high quality Al/SiCp coatings have been deposited on ZE41 magnesium alloy by laser cladding using a HPDL. The effect of the laser parameters on the cladding geometry and the properties of the cladding have been investigated.

## 2. Experimental methods.

ZE41 magnesium alloy was used as the substrate for laser cladding (chemical composition in Table 1), which was cut to the dimension of 250 x 250 x 5 mm<sup>3</sup>. Al - 35wt%SiCp composite powder was used as cladding material. Aluminum of the composite matrix was an Al12wt%Si alloy (powder properties in Table 2). The surface of the substrates was prepared by chemical attack with H<sub>2</sub>SO<sub>4</sub> 10%vol. solution.

Table 1. Chemical composition of ZE41 magnesium alloy.

Product	Chemical Composition (nominal weight %)			
	Zinc	Rare Earths	Zirconium	Magnesium
ZE41	3.5-5.0	0.8-1.7	0.4-1.0	Balance

Table 2. Powder properties.

Product		D50 (μm)	ρ (g·cm <sup>-3</sup> )
Al12wt.%Si	Metco 52C-NS	71	2.7
SiC	Navarro S.A F-360	26.2	2-2.25

The coating process were carried out with precise laser cladding system that consist of a 1300 W continuous wave diode laser (ROFIN DL013S) with a wavelength of 808-940 nm. Powder was projected coaxially with the laser beam trough a coaxial nozzle Fraunhofer IWS COAX 8. The powder focus is 13 mm

below the nozzle tip. Argon at 4.5 atm pressure and  $0.05 \text{ L}\cdot\text{s}^{-1}$  flow rate was used as a carrying gas. In all the experiments, the flow rate of carrying gas was kept constant. Hot-plate connected to temperature control system was used as substrate's support.

First, single-pass test of Al/SiCp on ZE41 have been performed. After, multi-pass test has been performed to do a complete coating; in these tests the optimum distance between consecutive laser lines was evaluated. The laser cladding process control parameters used were: laser power (500, 600, 650 and 700W); scan speed (3, 8, 14 and 17 mm/s); and focal position (-5, 0 and +5 mm). The influence of the focal position of the laser beam was evaluated. Fig. 1 shows a scheme of laser cladding in different focus modes.

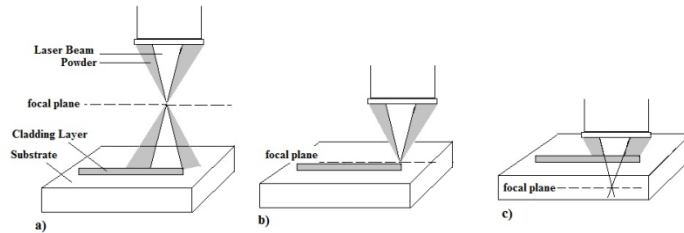


Fig. 1. Schematic of laser cladding in different focus modes. (a) positive defocus manner; (b) focus manner; (c) negative defocus manner.

To evaluate the influence of the laser cladding process control parameters in the coating properties, different output parameters were evaluated: aspect ratio between height and width of the track, melted zone depth, dilution zone depth, presence of interface pores and cracks, and reactivity between SiC particles and molten aluminum. These parameters were evaluated by image analysis software (Leica Application Suite) on the captured images obtained by a light microscope (OM; Leica DMR) and by a Scanning Electron Microscope (SEM; Hitachi S-3400N).

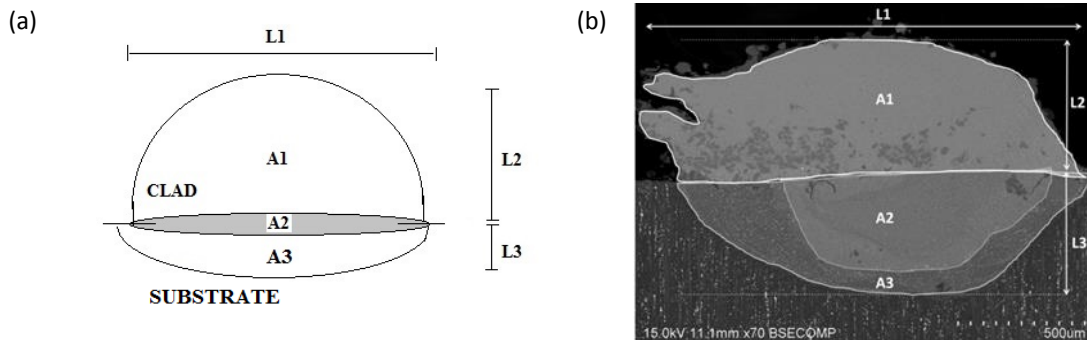


Fig. 2. Cross-section of a single laser cladding track; L1=width of the track; L2=height of the track; L3= depth of the substrate melted zone; A1= Cross-section area of the tracks; A2=cross-section area of the dilution substrate; A3= cross-section area of the melted substrate; (a) scheme; (b) real SEM micrographs.

Fig. 2 shows the cross-section scheme of a single laser cladding track and the real SEM micrographs, respectability. The aspect ratio was calculated through equation 1 using measurements obtained by image

analysis software. The melted depth zone was calculated directly by image analysis on the captures OM and SEM images. The dilution depth zone was calculated through equation 2 using measurements obtained by image analysis software. The presence of interface pores and cracks, and reactivity between SiC particles and molten aluminum was calculated directly using the phase expert module of the image analysis software, an example has shown in Fig 3.

$$\text{Aspect ratio} = \frac{L1}{L2} \quad (1)$$

$$\%Dilution = \frac{A2}{A1+A2} \quad (2)$$

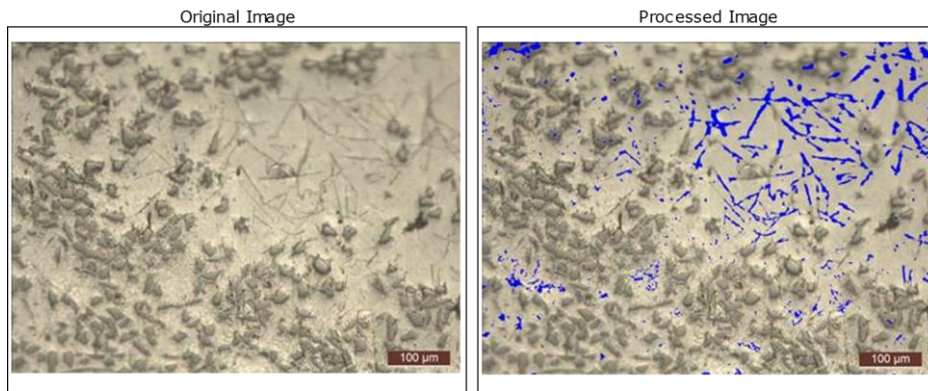


Fig. 3. Example of reactivity measurement using the phase expert module of the image analysis software.

Also, a Shimadzu microhardness tester was used to obtain a Vickers microhardness profile along the cross-section of the specimens. A load of 1 g for loading time of 15 seconds was used.

### 3. Results and discussion

Single laser track tests were carried out by changing the laser beam power, scanning speed and powder feeding rate. The cross sections (Fig. 4) show evidence the extreme sensitivity of the laser cladding coatings on both laser power and scan speed on the surface of the ZE41 magnesium alloy. Fig 4(a) shows the SEM micrographs of the different single-pass tests and the Fig. 4(b) shows the elements maps of these samples: the magnesium is color-coded in green, the aluminum in red, silicon in blue and carbon in cyan.

From the values measured on the cross sections, different contour maps were produced (Fig. 5) to illustrate the dependence of the output parameters on the laser power and laser speed. Green areas represent the most beneficial characteristics for a good-quality coating. For example, In Fig 5(a) green areas represent coatings with high aspect ratio and red areas represent coatings with low aspect ratio; in Fig 5(b) represent the coatings without reactivity in its microstructure and red areas represents the opposite. In Fig 5(c) green areas represent the good quality interfaces and in Fig 5(d and e) represent coatings with low molten and dilution zone depth, respectively. And finally, Fig 5(f) green areas represent coatings with high hardness and red areas represent coatings with low hardness.

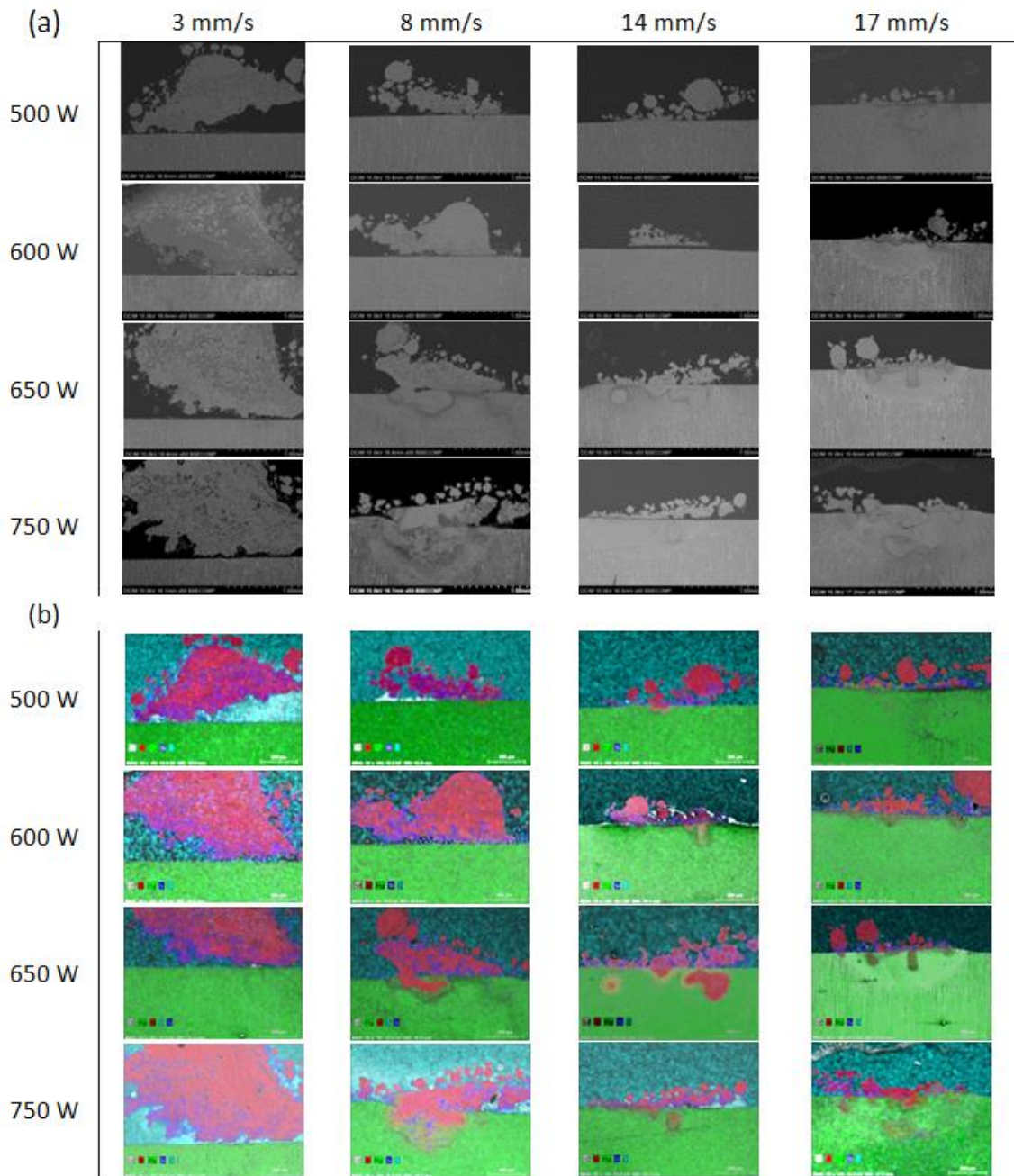


Fig. 4. Dependence of the cladding geometry for the laser beam, power and the scanning speed values. Cross-section scheme of a single laser cladding track. (a) SEM micrographs; (b) elements distribution map; Mg is color-coded in green, Al in red, Si in blue and C in cyan.

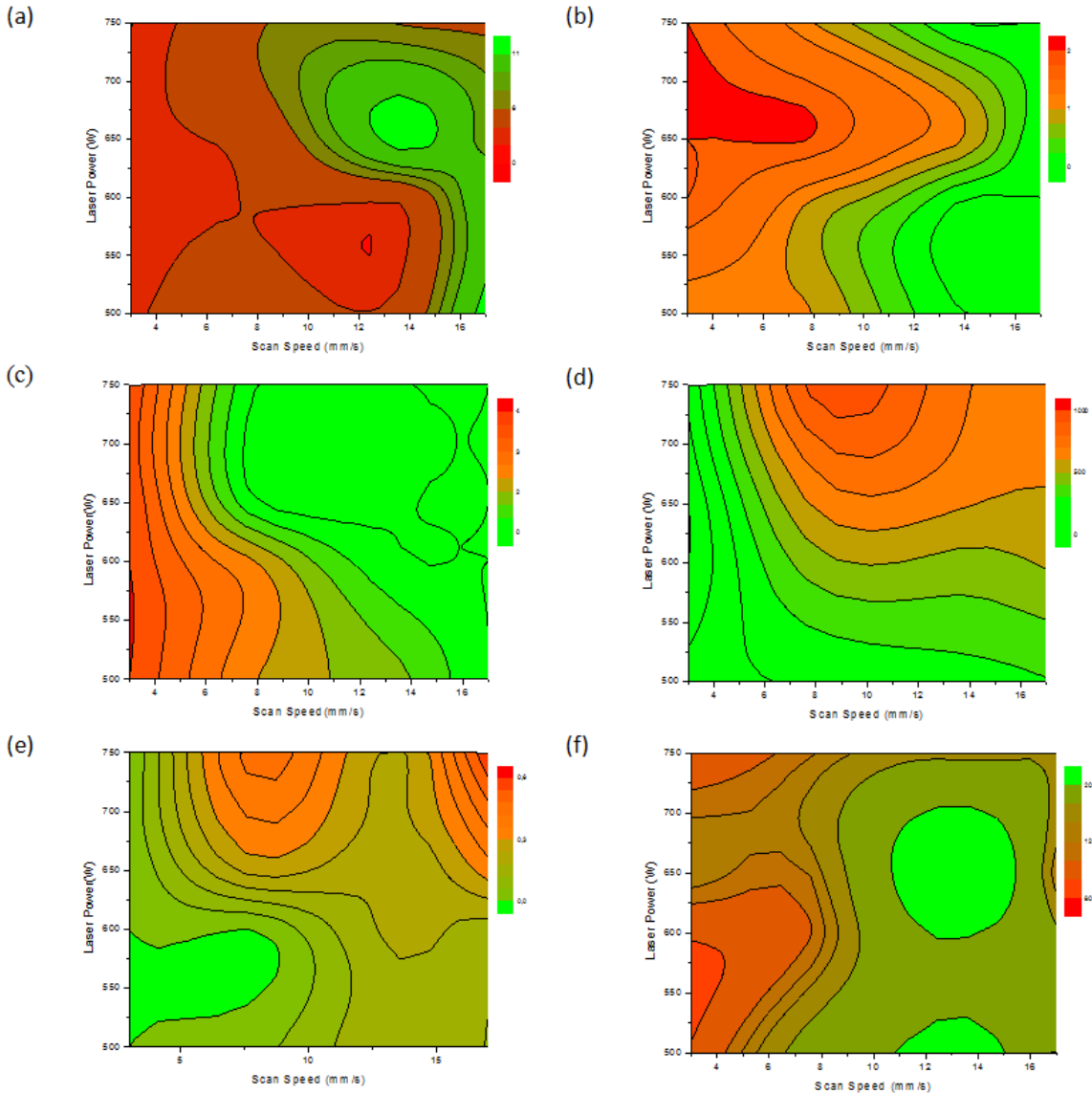


Fig. 5. Contour map of (a) aspect ratio; (b) reactivity between Al molten and SiC particles; (c) interface pores and cracks; (d) melted zone depth; (e) % Dilution; (f) microhardness ( $HV_{0.2}$ ) of the coating.

The aspect ratio increases with laser power and scan speed (Fig 5.a), although it gets its maximum at 650W and 14 mm/s, respectively. The desired aspect ratio depends on the application chosen, however, in most cases it is desirable to clad the surface with the lower number of laser passes (to get the largest width) and to avoid the formatting of pores in the overlapping zone, which improves as the height is reduced. Consequently, in most cases the aim is to get the highest ratio.

High reactivity zones overlap with low scan speed and high laser power (Fig. 5. b), which correspond with

the highest net energy input, for which higher temperatures are reached. This favors the kinetic and the interaction time of the reaction between SiC particles and molten aluminum. Furthermore, zones with more interface pores and cracks (Fig. 5. c) are higher at higher scanning speed, independently of the laser power because at higher scanning speed the substrate is less affected.

The evolution of the molten and the dilution depth zone is the opposite (Fig 5.d and e), are higher at higher laser power, independently of the scanning speed but in the case of the melted depth zone, at very low scan speed (less than 7mm/s) the molten depth zone is always low. The melted zone is a diffusive zone. In this case the diffusion flows were generated principally by Marangoni, Bouyancy and impact forces. Marangoni forces could produce upward flow in the center of the melted pool or in the melted pool wall. Bouyancy forces could produce that coldest materials flow to the interior of molten pool. In laser cladding process the temperature gradient is very high, so the molten pool walls are the coldest zone. Then, the magnesium substrate was dragged from molten pool walls to the interior of the molten pool zone by Bouyancy forces. And then, this magnesium fraction was dragged towards the coating (Park et al., 1997). This causes a mixture of magnesium substrate and aluminum coating matrix. The Mg increase improves the weldability between substrate and coating. For this reason, areas with higher dilution depth overlap with areas with less interface pores and cracks (Fig 5. d and e).

The coating hardening increases as the scanning speed increases and it is higher when the laser beam power has an intermediate value, getting its maximum 14 mm/s and 650 W, respectively (Fig. 5. f). These areas overlap with areas with less reactivity because the presence of  $Al_4C_3$  weakens the coating. These areas also overlap with areas with less interface pores and cracks and areas with higher dilution depth. Intermetallics formed into the dilution zones increases the substrates hardness. For this reason, substrates hardness changes along the melted zones and dilution zones, with respect to the original substrate's hardness.

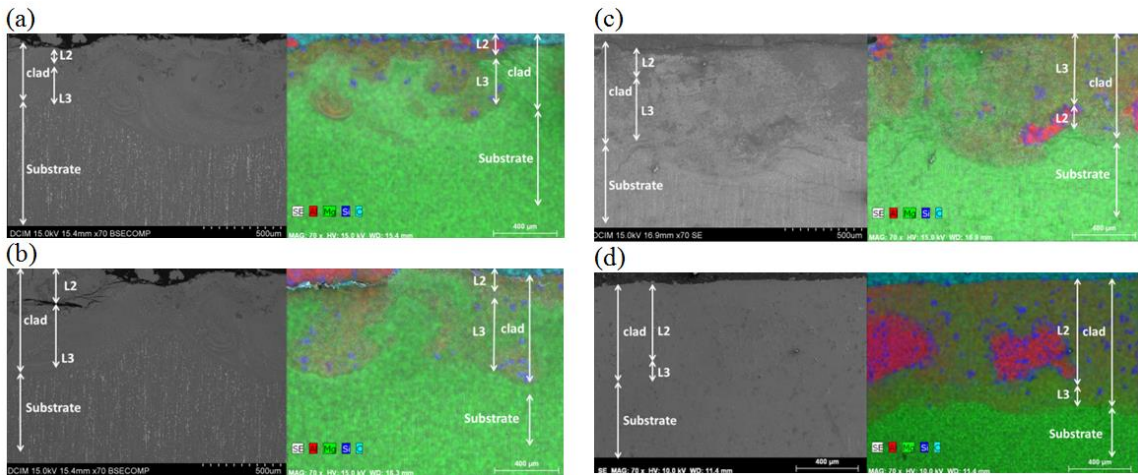


Fig. 6 Al/SiCp coating's elements distribution map obtained by EDX; Mg are color-coded in green, Al in red, Si in blue and C in cyan. Distance between consecutive laser lines: (a) 1.75mm; (b) 1.5mm; (c) 1.25mm; (d) 1mm.

The optimal set of parameters selected for laser cladding was 650 W for laser beam power and 17 mm/s for laser scanning speed. Multi-pass test has been performed to fabricate a complete coating; in these tests

the optimum distance between consecutive laser lines was evaluated. Fig 6 shows the SEM micrographs of the different multi-pass tests with different distance between consecutive lines, and its element maps obtained by EDX of the cross sections of these coatings. The magnesium is color-coded in green, the aluminum in red, silicon in blue and carbon in cyan. When the distance between consecutive lines is smaller than 1 mm there is not homogeneous dilution and there are aluminium free zones in the coating. The magnesium of the substrate was moving during the laser cladding due to the convection movement prior to the cooling of the molten pool; so, as smaller the distance between the laser lines as more homogenous is the Mg distribution into the coating, the coating is better deposited and the melted and heat affected zone are smaller.

To evaluate the coating microstructure, the cross-section of a multi-pass coating was analyzed by micrographs obtained by OM and SEM. The laser parameters used in it coating was 650 W for laser beam power, 17 mm/s for laser scanning speed and 1mm for distance between laser lines. The coating is a composite material constituted by SiC particles and magnesium intermetallic phases in an aluminum matrix. There were more SiC particles near the substrate-coating interface. The absence of reactivity between SiCp and molten aluminum may suggest that is caused because SiC particles are denser than Al12wt%Si (3.22 g/cm<sup>3</sup> and 1.3 g/cm<sup>3</sup> respectively). Increased Mg diffusion into the melt, forming Mg<sub>2</sub>Si dendrites and Mg-Al intermetallics, and Al<sub>4</sub>C<sub>3</sub> needles formation was avoided. There was not presence of primary silicon (N. Han et al.,1992; P.L. Ratnaparkhi et al., 1994; P. Volovitch et al., 2008). However, diffusion flows were not enough and lakes of aluminum matrix without Mg contents are formed. Al<sub>4</sub>C<sub>3</sub> needles were observed in these zones.

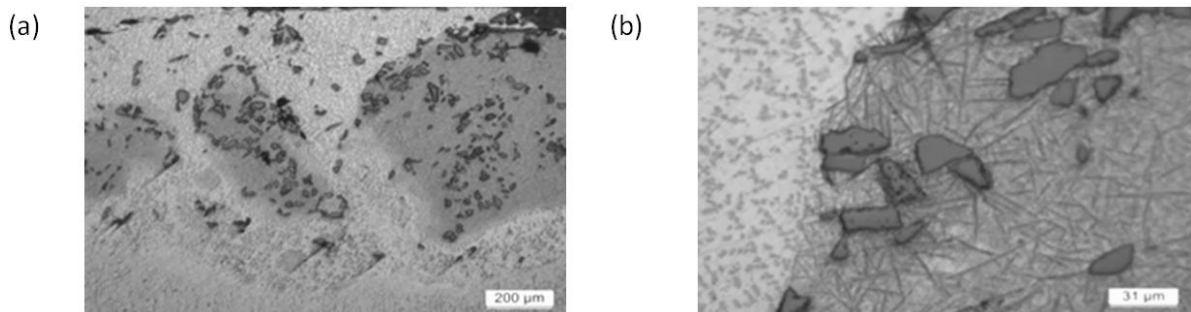


Fig. 7. OM Micrography of: (a) multi-pass Al/SiCp clad on ZE41; (b). Detail of Al/SiCp coating on ZE41.

The effect of the focus manner was analyzed. It was studied three different focus manner: on focus manner, negative defocus manner (-5mm from the focus manner) and positive focus manner (+5mm from the focus manner) Fig. 8. shows the schematic of cross-sections of multi-pass laser track and laser beam in different focus modes and its real SEM elements maps. The magnesium is color-coded in green, the aluminum in red, silicon in blue and carbon in cyan.

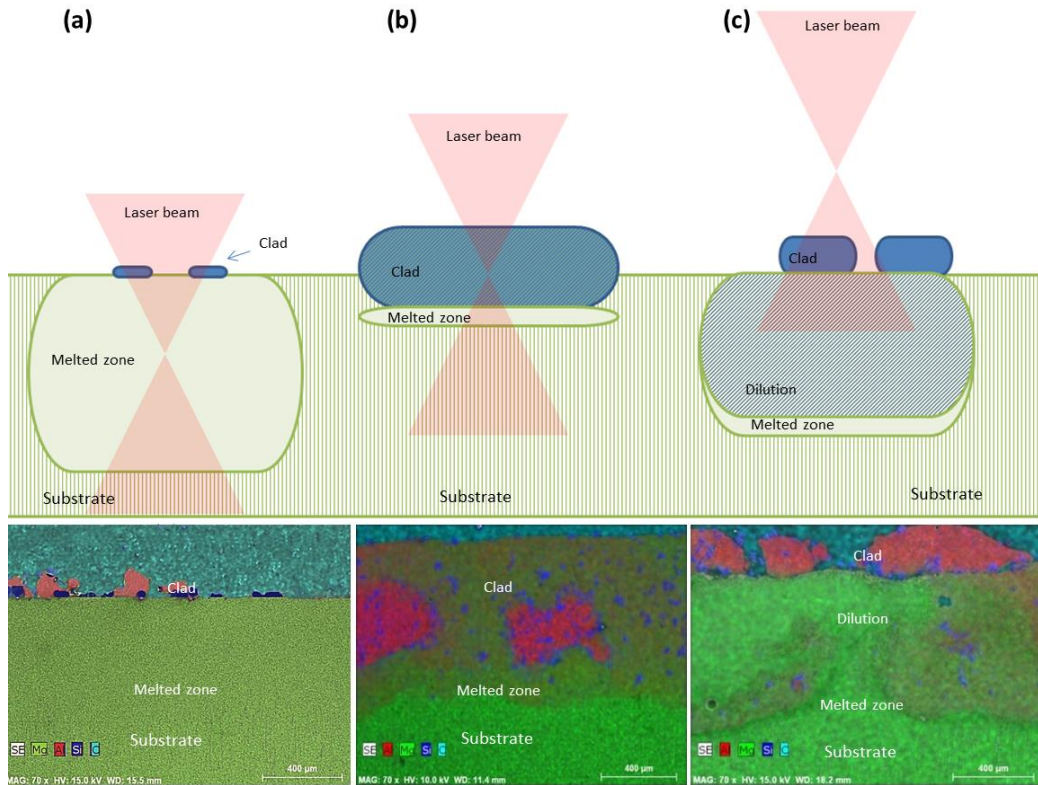


Fig. 8. Schematic of cross-sections of multipass laser track and laser beam in different focus modes and its real SEM elements maps. (a) negative defocus manner; (b) focus manner; (c) positive defocus manner.

Under the negative defocus condition (Fig. 8.a), the powder is only heated during its flights across the laser beam, never passing through the highest power zone of the beam, and not at the moment of its impact on the surface; so it tends to rebound away from the surface without melting and depositing. However, the net energy input inside the substrate is strong enough and its surface is highly influenced by it. The substrate shows a large fusion zone with a large molten depth and large heat affected zone. The heat affected zone has two different morphologies: a molten zone with dendritic grains and a recrystallization zone with grain growth, where the grain size is bigger. Under the focus condition, i.e. when the most part of the powder reaches the substrate surface when it is in the middle of the laser spot (fig. 8.b). In the moment of the impact of the powder with the surface, the laser quickly heats the powder and the substrate surface simultaneously. The hot powder is so plastic that achieves to keep contact with the surface during a long time, then the powder is melted and being deposited without rebound away. There is not a dilution zone but that the coating is skinning in the substrate. There is diffusion of magnesium from the substrate but the interface between coating and substrate is well defined. The heat affected zone has a very little depth and the grain size is intermediate between the grain sizes obtained in the HAZ in the other focus positions. Under the positive condition (fig. 8.c), the large fusion zone makes a high dilution rate. Some pores in the overlapping boundary zone closed to substrate can be observed. The substrate shows a large fusion zone with a large molten depth mixed with the dilution zone and little heat affected zone. The heat affected zone has grains with a little size big because there is recrystallization but there is not grain growth. Therefore, the smaller

height of the focus the smaller the dilution depth until in negative defocus manner there is not a dilution zone (there are only melted zone) because the powder rebound away against the surface.

#### 4. Conclusions

The results show evidence of the different characteristics of the laser cladding coatings using different laser power and scan speed on the surface of the ZE41 magnesium alloy. The optimal set of parameters selected for laser cladding was 650 W of laser beam power and 17 mm/s of laser scanning speed. An optimal distance between consecutive lines for multi-pass coatings was determined. When the distance between consecutive lines is less than 1 mm there is not homogeneous dilution and there are zones free from aluminium; so, as smaller the distance between the laser lines as more homogenous is the Mg distribution into the coating, the coating is better deposited and the melted and heat affected zone are smaller. Effect of the focus mode was determined. The smaller height of the focus the smaller the dilution depth until in negative defocus manner there is not a dilution zone (there are only melted zone) because the powder rebound away against the surface. The bigger height of the focus the bigger the dilution zone because of characteristics of the process the cooling is very fast and there is not grain growth as if there was in the case of negative defocus manner. The optimum height of the focus is the focus condition because the powder has melted by the laser beam and not rebound away the surface and the interface coating-substrate is the better. For the optimal conditions the coating, the optimal laser focus was the focus manner.

#### Acknowledgements

Authors wish to thanks the financial support of Ministerio de Economía y Competitividad (MAT2012-38407-C03-01) and Universidad Rey Juan Carlos.

#### References

- Zhong M., Liu W., 2010 Laser surface cladding: the state of the art and challenges, Proceedings of the Institution of Mechanical Engineers, Part C: Journal of Mechanical Engineering Science 224 (5) p 1041-1060.
- Liu Y.H., Guo Z.X., Yang Y., Wang H.Y., Hu J.D., Li Y.X., Chumakov A.N., Bosak N.A. 2006. Laser (a pulser Nd:YAG) cladding of AZ91D magnesium alloy with Al and Al<sub>2</sub>O<sub>3</sub> powders. Applied Surface Science. 253 p 1722-1728.
- Lee H-K. 2008. Effects of the cladding parameters on the deposition efficiency in pulsed Nd:YAG laser cladding. Journal of materials processing technology. 202 pp 321-327.
- Sun Y., Hao M., 2012. Statical analysis and optimization of process parameters in Ti6Al4V laser cladding using Nd: YAG laser. Optics and Lasers in Engineering. 50. P 985-995.
- Gao W., Zhao S., Liu F., Wang Y., Zhou C., Lin X. 2014. Effects of defocus manner on laser cladding of Fe-based alloy powder. Surface – Coatings. 248 p 54-62.
- Michael M. Avedesian and Hugh Baker. 1999. Magnesium and magnesium alloys. ASM Specialty Handbook. Editor: ASM International. Materials Park, OH.
- Hooker J.A., Doorbar P.J., 2000. Metal matrix composites for aeroengines, Journal of Materials Science & Technology. 16 p 725–731.
- Shibata K., Ushio H., 1994. Tribological application of MMC for reducing engine weight, Tribology International. 27 (1) p 39–44.
- Ureña A., Rodrigo P., Gil L., Escalera M.D., Baldonado J.L., 2001. Interfacial reactions in an Al–Cu–Mg/SiCw composite during liquid processing. Part I. Casting, Journal of Materials Science. 36 p 419–428.
- Park J., Lucas J. P. 1997. Moisture effect on SiCp/6061/Al MMC: dissolution of interfacial Al<sub>4</sub>C<sub>3</sub>. Scripta Materialia. 37 p 511-516.
- Han N., Pollard G., Stevens R. 1992. Microstructural Characterization of Sand Cast Aluminium alloy A356-SiC Particle Metal Matrix Composite. Materials Science and Technology. 8 p 52-56.
- Ratnaparkhi P.L., Howe J.M. 1994. Characterization of a Diffusion-Bonded Al-Mg Alloy/SiC Interface by High Resolution and Analytical Electron Microscopy. 25p 617-627
- Volovitch P. Masse J.E., Fabre A., Barrallier L., Saikaly W. 2008. Microstructure and corrosion resistance of magnesium alloy ZE41 with laser surface cladding by Al-Si powder. 202 p 4901-4914.